

Magma ponding in the Karakoram shear zone, Ladakh, NW India

Roberto F. Weinberg[†]

Geordie Mark*

Henning Reichardt

School of Geosciences, Monash University, Clayton, VIC 3800, Australia

ABSTRACT

Granitic melt migration and pluton emplacement are commonly closely associated with transcurrent shear zones. The processes that link granites to shear zones are not yet fully understood. The dextral-transpressive Karakoram shear zone in Ladakh, NW India, exposes anatectic rocks where synkinematic melt migration and ponding at kilometer scale were controlled by competency contrasts. Metasedimentary rocks and a dominantly granodioritic calc-alkaline intrusion underwent fluid-present partial melting at upper-amphibolite facies to produce leucogranite sheets and irregular intrusive masses dated at 21–14 Ma. Leucogranitic magmas ponded in the low-pressure strain shadow of the competent granodioritic calc-alkaline pluton, giving rise to (a) migmatitic rocks that are pervaded by irregular leucogranite intrusions at a scale of meters or tens of meters, and (b) the growth of the Tangtse pluton, a kilometer-scale sheeted complex. Thus, magmas accumulated during shearing and anatexis in a low-pressure strain shadow within the Karakoram shear zone. This magma provided a readily available magma source that could have been tapped to feed larger plutons at shallower levels by modifications in the pressure distribution accompanying changes in shear zone geometry and kinematics. We conclude that shear zones tapping anatectic regions act as magma pumps, creating and destroying magma traps at depth as they evolve, and leading to incremental magma addition to upper-crustal plutons.

Keywords: shear zone, magma emplacement, magma transport, strain shadow, sheeted complex, leucogranite, Karakoram.

[†]E-mail: Roberto.Weinberg@sci.monash.edu.au

*Present address: Haywood Securities Inc., 400 Burrard Street, Vancouver, British Columbia V6C 3A6, Canada.

INTRODUCTION

Plutons are commonly associated with transcurrent shear zones, where they display a number of characteristic three-dimensional (3-D) shapes (Brown and Solar, 1999; D'Lemos et al., 1992; Elias-Herrera and Ortega-Gutiérrez, 2002; Lacroix et al., 1998; McCaffrey, 1992; Roman-Berdiel et al., 1997; Tikoff and Teysier, 1992; Vigneresse, 1995; Weinberg et al., 2004). The close temporal and spatial association between synkinematic granitic plutons and crustal-scale transcurrent shear zones suggests a causative link between the two (Hutton and Reavy, 1992). Either shear zones control ascent and emplacement of granitic magmas (Brown and Solar, 1998b; Weinberg et al., 2004), or magma emplacement triggers nucleation of shear zones (e.g., Neves et al., 1996). The hypothesis that shear zones control the ascent and emplacement of granitic plutons is supported by mesoscale structures in migmatites (e.g., Brown and Solar, 1999; Sawyer, 1999) and is generally ascribed to the ability of shear zones to accommodate magma influx in extensional jogs, as well as higher permeability, temperature, and strain rate in shear zones (e.g., Brown and Solar, 1998a; D'Lemos et al., 1992; Leloup et al., 1999; Pe-Piper et al., 1998).

Weinberg et al. (2004) suggested that low mean pressure zones that develop at the shoulders of shear zones close to regional rheological contacts control the emplacement of magma bodies. Mancktelow (2006) argued for brittle behavior in ductile shear zones to account for the low mean pressure implied by widespread evidence that shear zones act as fluid or magma channels. Most studies of pluton–shear zone relationships explore the system at emplacement levels, away from the magma source. This is partly because significant magma accumulations are rare in regions of crustal anatexis (Brown, 2004). The lack of such accumulations implies that there is either an efficient mechanism to drain diffuse magma in the source (Rabinowicz and Vigneresse, 2004), or that magma accumulations in the source are only transient features.

This paper explores a rare magma accumulation within anatectic rocks presumed to be a part of the magma source region for the leucogranitic, 20–15 Ma Karakoram batholith (Weinberg et al., 2000). These anatectic rocks are exposed within the 7-km-wide, dextral-transpressive Karakoram shear zone, in Ladakh, NW India (Weinberg and Mark, 2008). These magma accumulations provide an opportunity to explore simultaneously the controls on magma migration and accumulation within source regions, and the ways in which shear zones control magma migration.

KARAKORAM SHEAR ZONE AND THE PANGONG METAMORPHIC COMPLEX

The ~800-km-long Karakoram shear zone is part of a set of faults that accommodate the northward movement of India (e.g., Avouac and Tapponnier, 1993). The Tangtse gorge in Ladakh (Fig. 1) cuts transversally across the shear zone and the Pangong Range, both of which trend on average N40W, and ~7 km wide, exposing upper-amphibolite-facies rocks of the Pangong metamorphic complex (Table 1) (Rolland and Pêcher, 2001). The shear zone in this area is divided into a number of high-strain, mylonitic strands. The Tangtse strand (Fig. 1) dips 70°NE, with lineations plunging 20–40°N, defining a dextral thrust, separating the overriding Pangong metamorphic complex to the NE from the down-thrusted Cretaceous Ladakh batholith and contemporaneous Khardung volcanics to the SW (Weinberg et al., 2000). The Pangong strand is a subvertical dextral shear zone, at least 2 km wide that separates the Pangong metamorphic complex from the Karakoram metamorphic complex to the NE (Fig. 1; Table 1). The Pangong Range, bounded by these two strands, is dominated by pure shear deformation characterized by NW-plunging, upright folds, trending N40W to N60W (Weinberg and Mark, 2008). This range is traversed by simple shear bands defined by intense dextral mylonitic foliation (Figs. 2 and 3) and well-defined stretching lineation plunging 30–40°NW (Weinberg et al., 2000).

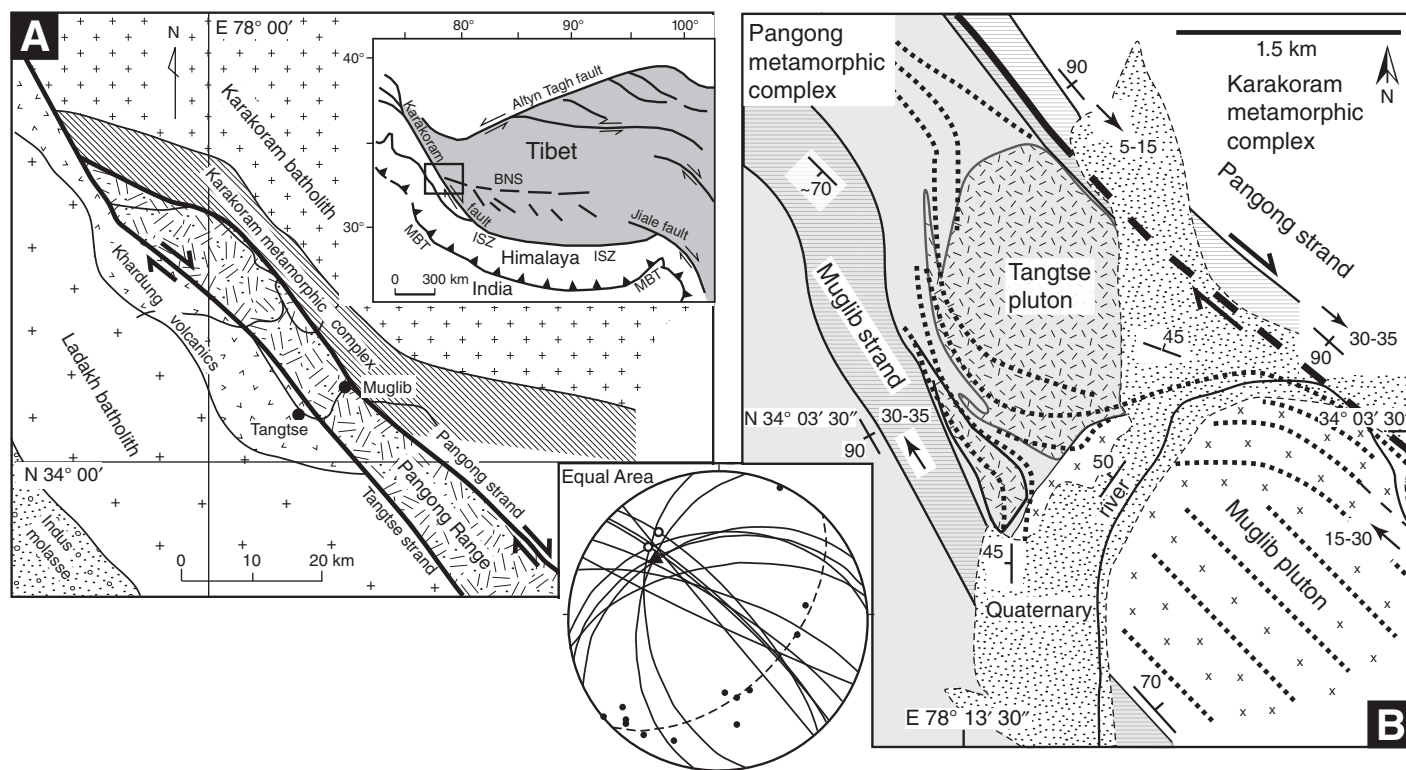


Figure 1. (A) Regional geological map of the Pangong Range where the Pangong metamorphic complex is exposed in Ladakh, NW India. The filled circle marked Muglib indicates the area covered in (B). (B) Geological map of the NE end of Tangtse gorge, where the Pangong strand of the Karakoram shear zone bounds the leucogranite Tangtse pluton and the older, calc-alkaline Muglib pluton. The Tangtse pluton is part of a sheet injection complex emplaced where the regional foliation (thick dashed lines) drapes around the NW-plunging nose of the competent Muglib pluton, defining a pressure shadow. The Muglib strand is not shown in (A). Leucogranites result from crustal anatexis as evidenced by migmatites exposed in the Tangtse gorge. Inset: Lower-hemisphere stereonet projection of foliation attitude (great circles) around the Muglib nose. Poles to foliation planes define a great circle (dashed line) and a fold axis plunging moderately NW (filled triangle), parallel to regional stretching lineations and outcrop-scale fold axes (white circles). MBT—Main Boundary thrust; ISZ—Indus suture zone; BNS—Bangong-Nujiang suture.

TABLE 1. SUMMARY OF ROCK SEQUENCES

Field Name	Lithologies
Tangtse pluton and leucogranite sheets	21–14 Ma sheeted leucogranite pluton (Fig. 3A). Leucogranites grade to leucotonalites and are composed of varying proportions of K-feldspar, plagioclase, quartz, garnet, muscovite, biotite, hornblende, and tourmaline. Inherited zircon cores have been dated at ca. 63 Ma and ca. 106 Ma (Searle et al., 1998; Weinberg et al., 2000; Weinberg and Searle, 1998).
Muglib pluton	118 ± 15 Ma (Ravikant, 2006) calc-alkaline batholith composed primarily of medium- to coarse-grained granodiorite (Figs. 4A and 4B), and minor quartz diorite and fine-grained biotite granite (border facies).
Pangong metamorphic complex	Upper-amphibolite facies (Rolland and Pêcher, 2001), anatectic sequence of biotite schist, psammites (Fig. 4C), and amphibolites interlayered with calc-silicate bands up to several hundred meters wide. All are intruded by granodiorites and granites interpreted to be related to the Muglib pluton (Weinberg and Mark, 2008).
Biotite-hornblende metaclastic sequence	Part of the Pangong metamorphic complex. Sequence ranges from biotite schists and psammites to amphibolites, depending on the modal contents of biotite, hornblende, quartz and plagioclase.
Karakoram metamorphic complex	Crops out to the northeast of the Karakoram shear zone; composed of biotite schists, amphibolites, and marbles. Lower-amphibolite facies, minor leucogranite intrusions and no evidence for migmatization. It differs from the Pangong metamorphic complex by the presence of marble layers, rarity of leucogranites, and lower metamorphic facies (Weinberg and Mark, 2008).
Karakoram batholith	Ca. 20–15 Ma, two-mica, tourmaline, garnet-bearing leucogranite body cropping out along the Shyok and Nubra valleys, N-NNW from the study area (Weinberg et al., 2000).
Ladakh batholith and Khardung volcanics	70–50 Ma calc-alkaline batholith and its volcanoclastic overburden, part of the Transhimalayan batholith (Dunlap and Wysoczanski, 2002; Weinberg and Dunlap, 2000), composed of gabbros through to granites. Crops out parallel to and south of the Karakoram shear zone.

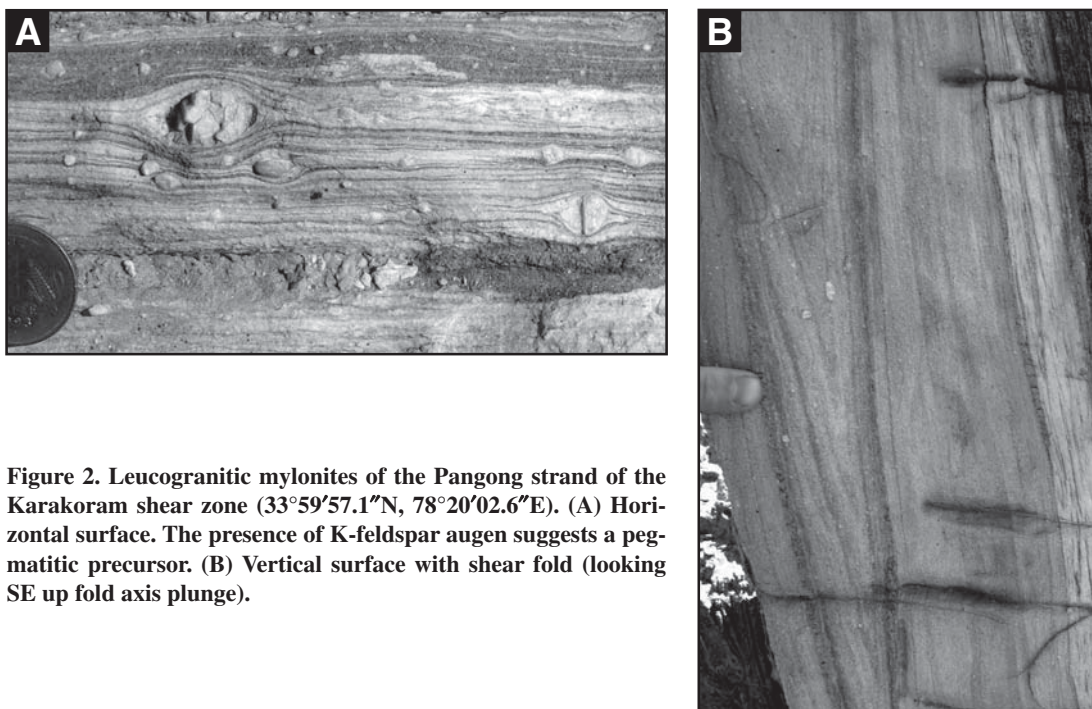


Figure 2. Leucogranitic mylonites of the Pangong strand of the Karakoram shear zone ($33^{\circ}59'57.1''\text{N}$, $78^{\circ}20'02.6''\text{E}$). (A) Horizontal surface. The presence of K-feldspar augen suggests a pegmatitic precursor. (B) Vertical surface with shear fold (looking SE up fold axis plunge).

The sequence of rocks comprising the Pangong metamorphic complex is described in Table 1. Rolland and Pêcher (2001) estimated upper-amphibolite conditions for rocks from this part of the complex, with peak temperatures around 700–750 °C and pressures of 4–5 kbar. During metamorphism, the biotite-rich end member of its metaclastic sequence is interpreted to have melted in situ without obvious peritectic minerals. Hornblende-bearing rocks are interpreted to have undergone similar melting and produced euhedral, poikilitic hornblende. Melting is inferred to have occurred at the wet solidus for these rocks, involving H₂O as a free phase, where biotite was stable, and new hornblende was either a peritectic product (Berger *et al.*, 2008; Lappin and Hollister, 1980) or a result of magmatic crystallization. Layer-parallel leucosomes are linked continuously to axial-planar leucosomes, giving rise to leucogranite and pegmatite dikes, sheets, and plutons, which intrude all major rock types (Weinberg, 1999; Weinberg and Searle, 1998). Because of the continuous link from leucosomes to larger dikes and plutons, we interpret that, at least in part, leucogranites are locally derived magmas (Weinberg and Mark, 2008).

The Tangtse strand is generally characterized by amphibolite-facies mylonites with a strong, gently NW-plunging lineation. The Pangong strand has an early amphibolite facies stretching lineation that plunges from horizontal to moderately NW, indicative of dextral movement with a NE-side-up component. Locally it is over-

printed by narrow zones of greenschist-facies retrogression with stretching lineation plunging SE, also indicative of dextral movement but with a NE-side-down component. A kinematic change from amphibolite- to greenschist-facies deformation was also documented further SE in Tibet along the shear zone (Valli *et al.*, 2007, 2008), where greenschist-facies shearing also was accompanied by a NE-side-down component (Lacassin *et al.*, 2004).

Amphibolite-facies mylonites are characterized by: (1) sheared leucogranites and pegmatites (Fig. 2), (2) biotite-plagioclase-quartz schists and psammities, with minor muscovite, or (3) competent boudins of hornblende-biotite-plagioclase-quartz amphibolites. Greenschist-facies retrogression is characterized by sheared (1) muscovite-biotite-plagioclase-quartz schists, where the muscovite makes up 50% of micas, and (2) mafic rocks composed of tremolite-actinolite, chlorite, biotite, plagioclase, quartz, plus minor muscovite and calcite. Detailed studies of deformation mechanisms of rocks from this shear zone have concluded that there is a range of fault rocks from ductile to brittle, including cataclastic rocks and clay-bearing fault gouges (Phillips and Searle, 2007; Rutter *et al.*, 2007).

K-Ar dating reveals that the Ladakh batholith, SW of the Pangong Range, had cooled significantly by ca. 36 Ma and was locally reheated in the vicinity of the Karakoram shear zone as a result of overthrusting of the Pangong metamorphic complex (see Dunlap *et al.* [1998] for a full dis-

ussion). The Karakoram metamorphic complex, NE of the Pangong Range, is composed of marbles, calc-silicate rocks interlayered with amphibolites, schists, and fine-grained slates (Dunlap *et al.*, 1998). Their mineral parageneses are indicative of lower-amphibolite facies, where schists lack evidence for partial melting and are composed of muscovite, biotite, plagioclase, quartz, cordierite, and garnet.

Leucogranite samples from within the Tangtse gorge yielded U-Pb zircon crystallization ages between 21 and 14 Ma (Phillips *et al.*, 2004; Searle *et al.*, 1998). Two leucogranite samples yielded two inherited zircon age groups: ca. 63 Ma and ca. 106 Ma, consistent with low-temperature remelting of rocks related temporally to the calc-alkaline Ladakh batholith (e.g., Weinberg and Dunlap, 2000; Weinberg *et al.*, 2000). The calc-alkaline rocks that are exposed in the gorge forming the Muglib pluton, which is interpreted to have undergone partial melting (see following) are the most likely source of these inherited zircons, as indicated by our unpublished zircon and sphene, U-Pb sensitive high-resolution ion microprobe (SHRIMP) ages, and by Rb-Sr geochronology (Ravikant, 2006).

CALC-ALKALINE MUGLIB PLUTON AND LEUCOGRANITE TANGTSE PLUTON

In the NE corner of the Tangtse gorge, leucogranitic rocks form an injection complex, which includes a sheeted pluton at the contact

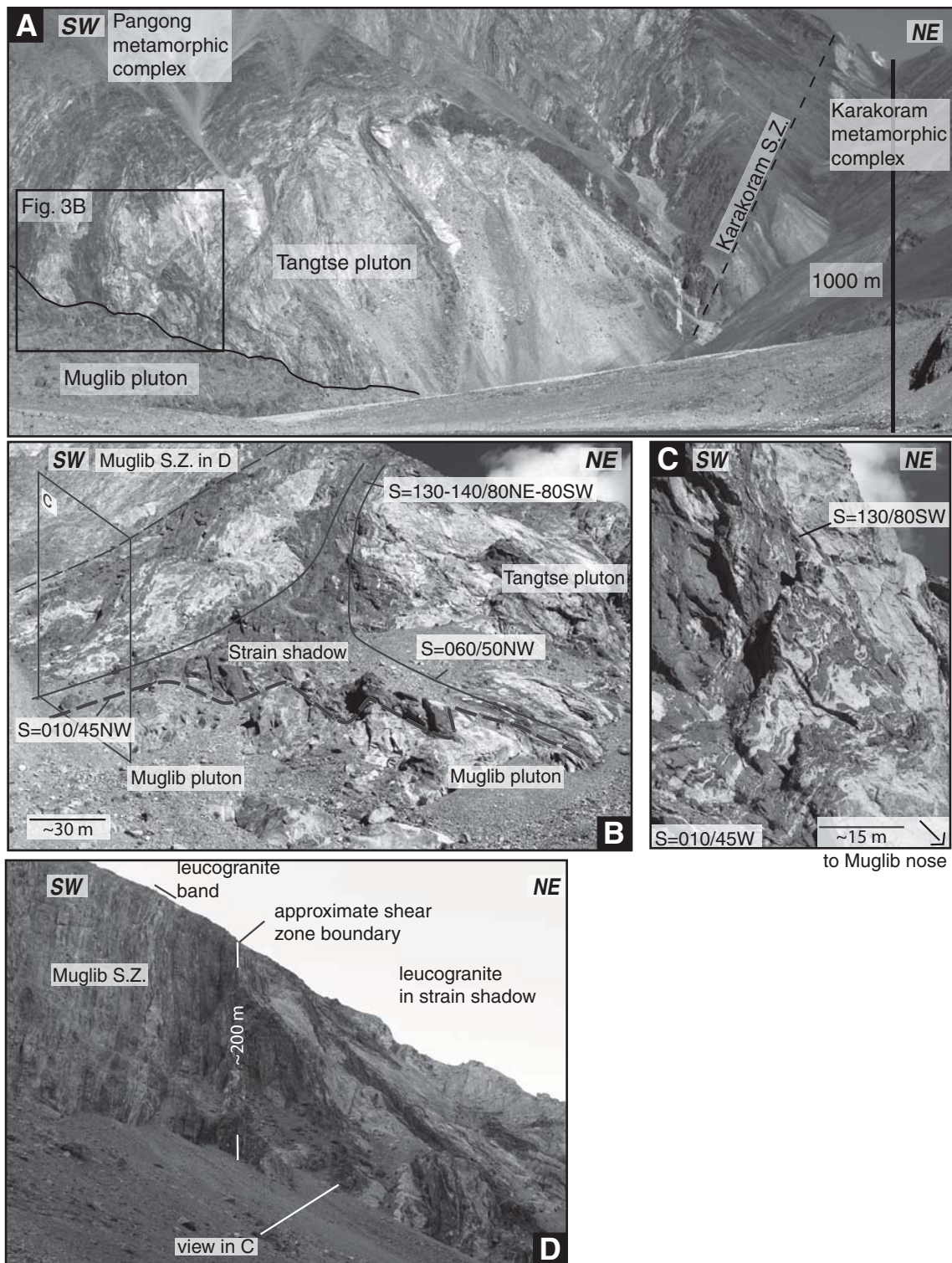


Figure 3. (A) Tangtse pluton NW of the Muglib pluton ($34^{\circ}03'30''\text{N}$, $78^{\circ}14'00''\text{E}$) showing dark screens of country rock within the pluton, and boudinaged leucogranite dikes in the distance, NW of the pluton and parallel to the dextral Pangong strand of the Karakoram shear zone, on the right-hand-side. All rocks are strongly sheared. The plane identified as the shear zone marks the contact between a mylonitic marble to the NE and strained migmatitic metasedimentary rocks intruded by leucogranite dikes to the SW. S.Z.—shear zone. Box on the left represents approximate position of B. (B) Foliation triple point resulting from the bifurcation of the regional trend around the NW termination of the Muglib pluton. (C) Irregular leucogranite sheets and pods on the SW of B where the regional foliation curves around the Muglib pluton. Photograph is looking NE. (D) Muglib strand characterized by intensely foliated rocks marking the SE boundary of the pressure shadow. The boundary of the shear zone is marked by two short white lines; a narrow band of leucogranite within the shear zone is also marked.

of the calc-alkaline Muglib pluton (Fig. 1B; Table 1). This area is bounded by the Pangong strand to the NE and the Muglib strand to the SE (Fig. 3D). The Muglib pluton is an elongate body trending parallel to the Pangong strand for at least 15 km. Close to the Muglib village, the northern contact is exposed where this pluton plunges under metasedimentary rocks and leucogranites, and defines a closure referred to here as the Muglib nose (Fig. 1B). The main facies of the Muglib pluton is a sheared medium- to coarse-grained biotite-hornblende

granodiorite that grades locally toward quartz-diorite and is intruded by leucogranitic dikes (Fig. 4A). Close to the NE margin, a medium-grained biotite-granite with local microdioritic enclaves defines a sheared, ~200-m-wide border facies. This facies forms dikes that intrude the country rocks and has narrow, foliation-parallel leucosomes with diffuse margins that lack melanosome rims. Leucosomes merge along the strike to form irregular coarse-grained leucogranitic patches, 10–30 cm wide, also with diffuse margins, such as in the boudin neck in

Figure 4B. This suggests that the leucosomes and leucogranitic patches are a result of in situ partial melting of the biotite-granite. By contrast, the main facies, although intruded by leucogranites (Fig. 4A), lacks widespread evidence for in situ melting. This anatexis is likely related to the regional 21–14 Ma anatexis that gave rise to leucogranites elsewhere, caused by the influx of a water-rich volatile phase (e.g., Fig. 4C; Weinberg and Mark, 2008).

Rocks of the Muglib pluton and country rocks have a strong penetrative solid-state foliation

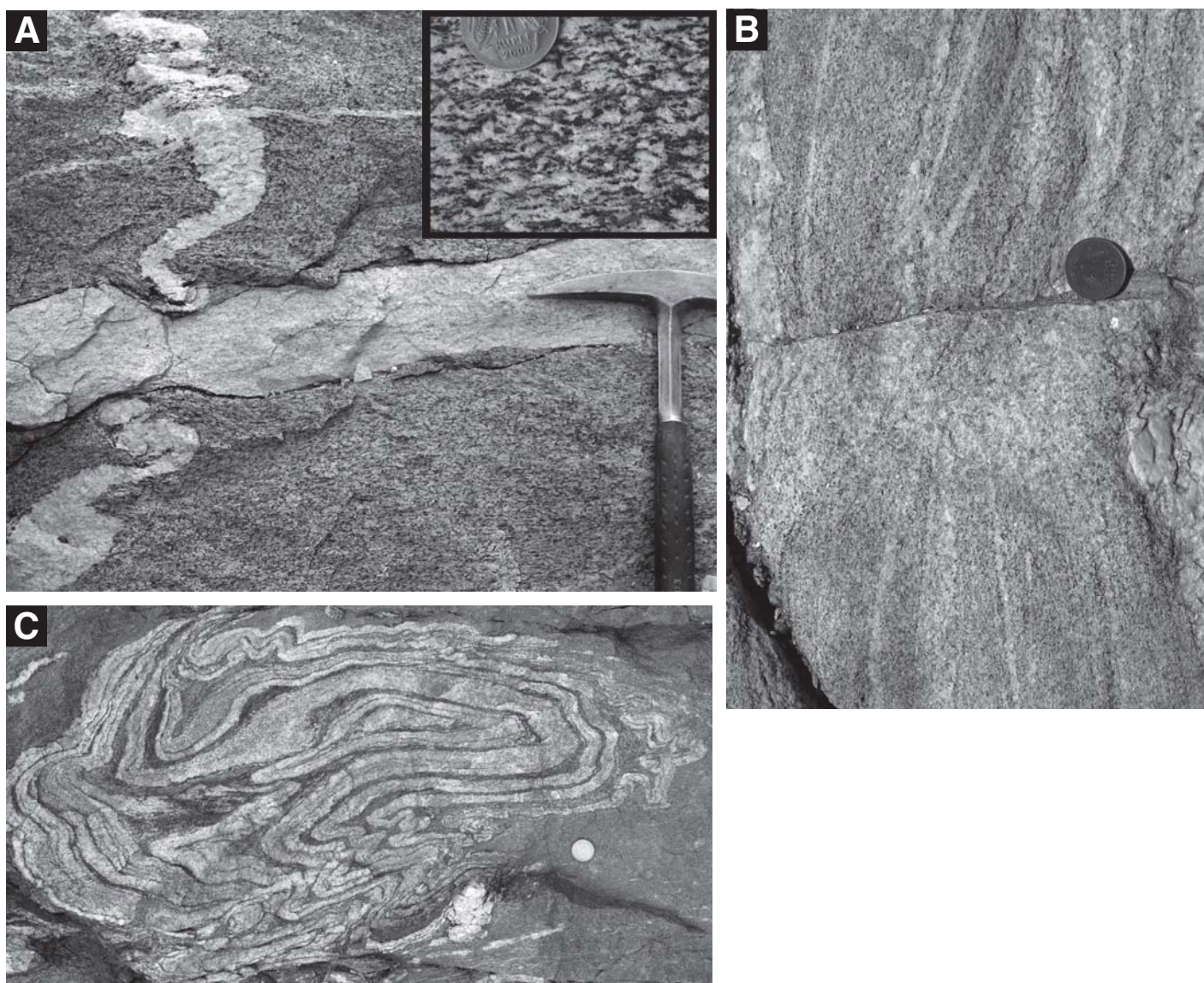


Figure 4. (A) Deformed granodiorite of the Muglib pluton intruded by pegmatitic leucogranite dikes, folded, and stretched. Inset: dextral shearing of granodiorite indicated by S-C-C' foliations. Both images are from nearly horizontal planes, and NW is to the right ($33^{\circ}59'05.0''\text{N}$, $78^{\circ}18'37.8''\text{E}$). (B) Medium-grained biotite-granite and leucosome layers with indistinct boundaries linked to a pod in the boudin neck. This is interpreted to indicate in situ melting during deformation. Horizontal exposure, NW is toward the top of the photograph. (C) Migmatitic biotite-psammite with chaotically folded layered leucosomes in steep exposure within the Tangtse pluton. Looking WNW, up is to the left ($34^{\circ}03'42.6''\text{N}$, $78^{\circ}13'52.2''\text{E}$).

(Fig. 4A) that strikes generally N40W, with variably steep dips, and lineation plunging moderately NW. Dextral shear deformation is indicated by S-C-C' fabric (Fig. 4A, inset), asymmetric folds, and asymmetric boudinage. Bedding in country rocks NE of the pluton is parallel to penetrative foliation and to the Pangong strand of the shear zone, but both deviate from that trend to drape around the Muglib nose, where they have moderate northerly dips (Figs. 1B, 3B, and 3C). Poles to foliation (Fig. 1, inset) in the Muglib nose define a great circle, from which a fold axis plunging moderately NW can be inferred. This is roughly parallel to both local and regional lineation (Weinberg et al., 2000) and to hinge lines of metric open folds mapped in the area.

Leucogranitic sheets and irregular pods crop out in the region of deflected foliation (Figs. 1 and 3) and occupy more than 50% of the surface area where they form an injection migmatite (Weinberg and Searle, 1998). The Tangtse pluton (Fig. 3A) was formed in this zone by the amalgamation of numerous leucogranite sheets. The pluton is 1.5 km long and is bounded by the Pangong strand to the NE. Its vertical exposure is ~600 m, and it is 200–300 m wide. The leucogranite sheets intrude older, fine- to medium-grained biotite-granite sheets, possibly related to the calc-alkaline Muglib pluton, and migmatitic biotite-hornblende metaclastic rocks that are preserved as screens inside the pluton (Figs. 3A and 3B). The regional foliation trend deflects not only around the Muglib pluton, but also around the northwestern end of the Tangtse pluton (Fig. 1B), implying that after solidification, it also behaved as a competent body during continued deformation. In the shear zones that surround the Muglib nose area, the volume of leucogranites is reduced to 10%–30% of the total. This is clear in the Muglib strand (Fig. 3D), where narrow, irregular bands of leucogranite are recognizable but less voluminous than away from the shear zone.

DISCUSSION

Contemporaneous Magmatism, Folding, and Dextral Shearing

Folds generally have steep axial-planar foliation striking between N60W to N40W, with NW-plunging fold axes (e.g., Fig. 4A; Weinberg and Mark, 2008). This fold geometry is compatible with the dominantly dextral shearing in the two NW-striking bounding strands of the Karakoram shear zone. Together, they account for transpression, which explains the large scale pop-up structure that characterizes the Pangong Range (Weinberg et al., 2000).

There is considerable discussion regarding the relative timing of melting and deformation

in the Karakoram shear zone. The geometries of leucosomes, representing what were once melt-rich parts of partially molten rocks, and folds demonstrate that melting took place during folding. For example, leucosomes parallel with migmatite layering merge continuously with leucosomes parallel to axial-planar foliation. Magma transfer through this leucosome network assisted folding (Weinberg and Mark, 2008). Evidence of contemporaneity between melting and dextral shearing can be found, but is obscured by subsequent subsolidus shearing (Dunlap et al., 1998; Rutter et al., 2007). Subsolidus deformation is reflected in variable strain intensities recorded by leucogranites as a function of grain size and as a function of their location in relation to high-strain zones. Leucogranites vary from virtually undeformed in coarse-grained pegmatitic portions, to weakly foliated in areas of folding, to fully recrystallized mylonites within shear zones (Figs. 2A and 2B). These foliations generally strike NW and dip steeply, and lineations in mylonitic leucogranites plunge NW, all of which are parallel to the shear zone fabric.

The outcrop at Tangtse Gompa, on the Tangtse strand of the shear zone (described in Phillips et al., 2004; Rutter et al., 2007), preserves evidence for the synkinematic intrusion of leucogranites. Here, the dominant strike of mylonitic foliation and lithologic layering is N70W, with a nearly vertical dip. A 20-cm-wide leucogranite dike intrudes a dextral brittle fault that strikes N-S, and displaces layering and mylonitic shear planes. This N-S-trending fault is kinematically compatible with the dextral shearing on the Tangtse strand, and the leucogranite that intrudes it records also a faint N70W-striking and steeply dipping foliation parallel to mylonitic foliation in surrounding rocks. These features suggest that dextral brittle faulting formed during shearing on the Tangtse strand and was exploited by a synkinematic leucogranite dike. Once solidified, the dike was overprinted by continued shearing.

In the same outcrop there are also layer-parallel leucogranite mylonitic bands, as well as leucogranitic dikes cutting across the main fabric at a variety of angles. When hosted by competent rocks, such as amphibolites, crosscutting dikes tend to be continuous and of regular width. However, when these dikes enter a less-competent rock type, such as marble, their trends deviate towards that of the shear zone orientation, in a manner consistent with increased straining. In the process, the dikes become strongly boudinaged, while, internally, they record varying bulk strain, from strongly deformed mylonites to apparently undeformed pegmatites. Strain in these magmatic rocks seems to decrease with decreasing age (Phil-

lips et al., 2004) but also decreases with increasing grain size. There are examples of folded dikes with apparently undeformed pegmatites coexisting in the same dike with strongly foliated medium-grained leucogranite. All the evidence in this outcrop is strongly suggestive of continued magma intrusion during shearing. This is at odds with conclusions by Phillips et al. (2004), but confirms a similar conclusion reached farther south along the shear zone in Tibet in rocks with a broadly similar history (Lacassin et al., 2004; Valli et al., 2007).

Thus, we conclude, based on: (1) the strain compatibility arguments, (2) the large-scale pop-up structure that exhumed the Pangong metamorphic complex (Weinberg et al., 2000), and (3) the evidence for synkinematic 21–14 Ma in situ melting and leucogranite intrusion, that all three events—folding, dextral shearing, and melting—were contemporaneous and related.

Pressure Shadow and Magma Accumulation

The large accumulation of younger leucogranitic rocks mapped immediately northwest and physically above the Muglib nose (Figs. 1 and 3) contrasts with the less voluminous leucogranite bands in the shear zones (Fig. 3D) including those that border the Muglib pluton. The irregular shape of leucogranite sheets and pods in the nose area, leading to the pervasive breakup of country rocks (Fig. 3C), suggests that this region was at temperatures above or close to magma solidus at the time of intrusion (Weinberg and Mark, 2008; Weinberg and Searle, 1998).

The deflection of the regional foliation trend around the Muglib pluton to drape around the Muglib nose (Fig. 1) is interpreted to result from the Muglib pluton behaving as a competent body during deformation. The deflection defines what is known as a foliation triple point (Johnson et al., 2003; Pons et al., 1995) and is associated with a low pressure strain shadow, like those developed around porphyroblasts. We argue that the magma accumulation resulted from migration and ponding driven by a negative pressure gradient into this zone. In this way, the older, competent Muglib pluton not only contributed with magma to the new pluton, as inferred from its partial melting and presence of inherited zircons in the leucogranites, but also created the conditions for growth of the younger pluton.

Magma Traps and Magma Pumping in Shear Zones

Shear zones can give rise to a number of low-pressure sites, not only in pressure shadows around competent rocks, but also in dilational

jogs (Fig. 5), pull-apart regions, shear zone terminations (Brown and Solar, 1998a; D'Lemos et al., 1992; Davies, 1982), or dilational areas resulting from active, crosscutting shear zones. These low-pressure sites form effective magma traps, and the volume of magma accumulated depends on: (1) the scale of the heterogeneity leading to low pressures, (2) pressure gradients driving melt into the low-pressure sites, which are a function of regional stresses, (3) the degree of partial melting and permeability of the system, and (4) the time available before the system is modified.

If the nature of strain and the distribution of stress in dilatant sites in shear zones are modified before magma solidification, traps can be destroyed, and magma accumulations can be pumped out, becoming available for pluton growth elsewhere in the system. Considering the evolving dynamic, kinematic, and geometric nature of large-scale tectonic systems, any particular shear zone in the system is likely to evolve through time. For example, changes in plate geometry, movement direction, or velocity will impact on the movement sense and stress distribution in shear zones. Shear zones are also sensitive to local block rearrangements. Furthermore, as the system evolves, the thermal profile and rock rheology around and within a shear zone will also change, triggering fluctuations in stress intensity and direction, changes in competency contrasts between rock types, and thus the nature of deformation and stress in and around the shear zones. All of these changes affect the stability of magma traps.

We postulate that magma traps are most likely transitory features that provide a temporary residence for magmas along their general upward migration. This is shown schematically in Figure 5, where a change from transtension to transpression is depicted. Tortuous shear zones that act to deform complex anatectic rock packages and undergo varied kinematic histories are likely to develop a number of such traps that can be created and destroyed during the history of the system. During periods of steady straining, magmas accumulate in traps with only minor leakage out of the anatectic zone (Fig. 5A). During periods of transition in the nature of straining, large volumes of melt are expelled from the anatectic shear zone (period between Figs. 5A and 5B) (e.g., Glazner, 1991). Each trap, and consequently each major magma batch being expelled, may have a distinct chemical signature that represents different proportions of magmas from different sources, degrees of partial melting and residuum separation.

In conclusion, shear zones may act as pumps by locally trapping magma in anatectic terranes until local or regional changes force the

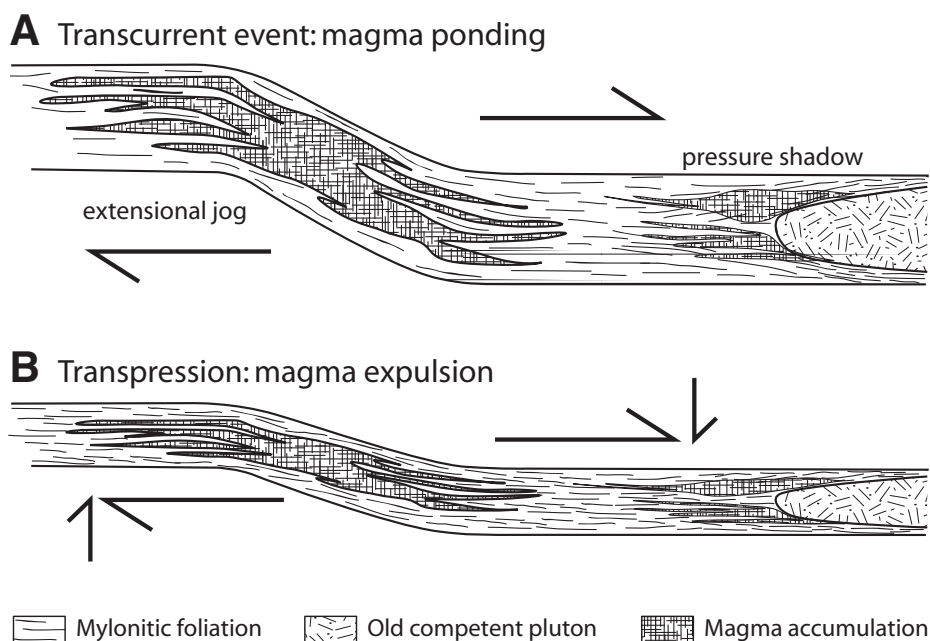


Figure 5. Magma accumulations in a shear zone. (A) During a transcurrent event, magma accumulates in dilational jogs or in strain shadows around competent bodies within an anatectic region. During this stage, minor volumes of magma leak out to the upper crust. (B) A change to transpression expels magma from these regions. The switch from a transcurrent to a transpressive regime leads to a magma pumping event. The change in regime exemplified here is one of a number of possibilities. Magma pumping will take place in any system, or part of a system, that changes from dilation to contraction. Repetitive pumping results from temporal fluctuation between these two states.

magma out, feeding batch growth of batholiths elsewhere. Major periods of magma pumping should accompany periods of changes in shear zone kinematics (D'Lemos et al., 1992). Thus, magma trapping in anatectic shear zones and shear pumping events during periods of change could explain incremental growth of complex plutons over millions of years (Coleman et al., 2004; Deniel et al., 1987; Mahan et al., 2003) punctuated by short periods of high magma flux (Matzel et al., 2006).

ACKNOWLEDGMENTS

We thank Andy Tomkins, Gary Solar, and Scott Patterson for reviews of an early version of this paper. We thank also Mike Brown, Jean-Louis Vigneresse, and Associate Editor Luca Ferrari for their detailed and constructive reviews.

REFERENCES CITED

- Avouac, J.-P., and Tapponnier, P., 1993, Kinematic model of active deformation in central Asia: *Geophysical Research Letters*, v. 20, no. 10, p. 895–898, doi: 10.1029/93GL00128.
- Berger, A., Burri, T., Alt-Epping, P., and Engi, M., 2008, Tectonically controlled fluid flow and water-assisted melting in the middle crust: An example from the Central Alps: *Lithos*, v. 102, 3/4, 598–615 doi:10.1016/j.lithos.2007.07.027.

- Brown, M., 2004, The mechanisms of melt extraction from lower continental crust of orogens: Is it a self-organized critical phenomenon?: *Transactions of the Royal Society of Edinburgh: Earth Sciences*, v. 95, p. 35–48, doi: 10.1017/S0263593300000900.
- Brown, M., and Solar, G.S., 1998a, Granite ascent and emplacement during contractional deformation in convergent orogens: *Journal of Structural Geology*, v. 20, no. 9–10, p. 1365–1393, doi: 10.1016/S0191-8141(98)00074-1.
- Brown, M., and Solar, G.S., 1998b, Shear-zone systems and melts: Feedback relations and self-organization in orogenic belts: *Journal of Structural Geology*, v. 20, no. 2–3, p. 211–227, doi: 10.1016/S0191-8141(97)00068-0.
- Brown, M., and Solar, G.S., 1999, The mechanism of ascent and emplacement of granite magma during transpression: A syntectonic granite paradigm: *Tectonophysics*, v. 312, p. 1–33, doi: 10.1016/S0040-1951(99)00169-9.
- Coleman, D.S., Gray, W., and Glazner, A.F., 2004, Rethinking the emplacement and evolution of zoned plutons; geochronologic evidence for incremental assembly of the Tuolumne Intrusive Suite, California: *Geology*, v. 32, no. 5, p. 433–436, doi: 10.1130/G20220.1.
- Davies, F.B., 1982, Pan-African granite intrusion in response to tectonic volume changes in a ductile shear zone from northern Saudi Arabia: *The Journal of Geology*, v. 90, no. 5, p. 467–483.
- Deniel, C., Vidal, P., Fernandez, A., LeFort, P., and Peucat, J.-J., 1987, Isotopic study of the Manaslu granite (Himalaya, Nepal): Inferences on the age and source of Himalayan leucogranites: *Contributions to Mineralogy and Petrology*, v. 96, p. 78–92, doi: 10.1007/BF00375529.
- D'Lemos, R.S., Brown, M., and Strachan, R.A., 1992, Granite magma generation, ascent and emplacement within a transpressional orogen: *Journal of the Geological Society of London*, v. 149, p. 487–490, doi: 10.1144/gsjgs.149.4.0487.

- Dunlap, W.J., and Wycoszanski, R., 2002, Thermal evidence for Early Cretaceous metamorphism in the Shyok suture zone and age of the Khardung volcanic rocks, Ladakh, India: *Journal of Asian Earth Sciences*, v. 20, p. 481–490.
- Dunlap, W.J., Weinberg, R.F., and Searle, M.P., 1998, Karakoram fault zone rocks cool in two phases: *Journal of the Geological Society of London*, v. 155, p. 903–912, doi: 10.1144/gsjgs.155.6.0903.
- Elias-Herrera, M., and Ortega-Gutiérrez, F., 2002, Caltepec fault zone: An Early Permian dextral transpressional boundary between the Proterozoic Oaxacan and Paleozoic Acatlán complexes, southern Mexico, and regional tectonic implications: *Tectonics*, v. 21, doi: 10.1029/2000TC001278.
- Glazner, A.F., 1991, Plutonism, oblique subduction, and continental growth; an example from the Mesozoic of California: *Geology*, v. 19, no. 8, p. 784–786, doi: 10.1130/0091-7613(1991)019<0784:POSACG>2.3.CO;2.
- Hutton, D.H.W., and Reavy, R.J., 1992, Strike-slip tectonics and granite petrogenesis: *Tectonics*, v. 11, no. 5, p. 960–967, doi: 10.1029/92TC00336.
- Johnson, S.E., Fletcher, J.M., Fanning, C.M., Vernon, R.H., Paterson, S.R., and Tate, M.C., 2003, Structure, emplacement and lateral expansion of the San Jose tonalite pluton, Peninsular Ranges Batholith, Baja California, Mexico: *Journal of Structural Geology*, v. 25, p. 1933–1957, doi: 10.1016/S0191-8141(03)00015-4.
- Lacassin, R., Valli, F., Arnaud, N., Leloup, P.H., Paquette, J.L., Haibing, L., Tapponnier, P., Chevalier, M.-L., Guillot, S., Maheo, G., and Zhiqin, X., 2004, Large-scale geometry, offset and kinematic evolution of the Karakoram fault, Tibet: *Earth and Planetary Science Letters*, v. 219, p. 255–269, doi: 10.1016/S0012-821X(04)00006-8.
- Lacroix, S., Sawyer, E.W., and Chown, E.H., 1998, Pluton emplacement within an extensional transfer zone during dextral strike-slip faulting: An example from the late Archaean Abitibi Greenstone Belt: *Journal of Structural Geology*, v. 20, no. 1, p. 43–59, doi: 10.1016/S0191-8141(97)00071-0.
- Lappin, A.R., and Hollister, L.S., 1980, Partial melting in the Central gneiss complex near Prince Rupert, British Columbia: *American Journal of Science*, v. 280, p. 518–545.
- Leloup, P.H., Ricard, Y., Battaglia, J., and Lacassin, R., 1999, Shear heating in continental strike-slip shear zones: Model and field examples: *Geophysical Journal International*, v. 136, p. 19–40, doi: 10.1046/j.1365-246X.1999.00683.x.
- Mahan, K.H., Bartley, J.M., Coleman, D.S., Glazner, A.F., and Carl, B.S., 2003, Sheeted intrusion of the synkinematic McDoyle pluton, Sierra Nevada, California: *Geological Society of America Bulletin*, v. 115, no. 12, p. 1570–1582, doi: 10.1130/B22083.1.
- Mancktelow, N.S., 2006, How ductile are ductile shear zones?: *Geology*, v. 34, no. 5, p. 345–348, doi: 10.1130/G22260.1.
- Matzel, J.E.P., Bowring, S.A., and Miller, R.B., 2006, Time scales of pluton construction at differing crustal levels: Examples from the Mount Stuart and Tenpeak intrusions; North Cascades, Washington: *Geological Society of America Bulletin*, v. 118, p. 1412–1430, doi: 10.1130/B25923.1.
- McCaffrey, K.J.W., 1992, Igneous emplacement in a transpressive shear zone: Ox Mountains igneous complex: *Journal of the Geological Society of London*, v. 149, p. 221–235, doi: 10.1144/gsjgs.149.2.0221.
- Neves, S.P., Vauchez, A., and Archanjo, C.J., 1996, Shear zone-controlled magma emplacement or magma-assisted nucleation of shear zones? Insights from northeast Brazil: *Tectonophysics*, v. 262, p. 349–364, doi: 10.1016/0040-1951(96)00007-8.
- Pe-Piper, G., Koukouvelas, I., and Piper, D.J.W., 1998, Synkinematic granite emplacement in shear zone: The Pleasant Hill pluton, Canadian Appalachian: *Geological Society of America Bulletin*, v. 110, no. 4, p. 523–536, doi: 10.1130/0016-7606(1998)110<0523:SGEIAS>2.3.CO;2.
- Phillips, R.J., and Searle, M.P., 2007, Macrostructural and microstructural architecture of the Karakoram fault: Relationship between magmatism and strike-slip fault: *Tectonics*, v. 26, p. TC3017, doi: 10.1029/2006TC001946.
- Phillips, R.J., Parrish, R.R., and Searle, M.P., 2004, Age constraints on ductile deformation and long-term slip rates along the Karakoram fault zone, Ladakh: *Earth and Planetary Science Letters*, v. 226, p. 305–319, doi: 10.1016/j.epsl.2004.07.037.
- Pons, J., Barbey, P., Dupuis, D., and Léger, J.M., 1995, Mechanisms of pluton emplacement and structural evolution of a 2.1 Ga juvenile continental crust: The Birimian of southwestern Niger: *Precambrian Research*, v. 70, p. 281–301, doi: 10.1016/0301-9268(94)00048-V.
- Rabinowicz, M., and Vigneresse, J.L., 2004, Melt segregation under compaction and shear channeling: Application to granitic magma segregation in a continental crust: *Journal of Geophysical Research*, v. 109, B04407, doi: 10.1029/2002JB002372.
- Ravikant, V., 2006, Utility of Rb-Sr geochronology in constraining Miocene and Cretaceous events in the eastern Karakoram, Ladakh, India: *Journal of Asian Earth Sciences*, v. 27, p. 534–543, doi: 10.1016/j.jseaes.2005.05.007.
- Rolland, Y., and Pêcher, A., 2001, The Pangong granulites of the Karakoram fault (western Tibet): Vertical extrusion within a lithosphere-scale fault?: *Comptes Rendus de l'Académie des Sciences, Serie II, Fascicule A—Sciences de la Terre et des Planètes*, v. 332, no. 6, p. 363–370.
- Roman-Berdiel, T., Gapais, D., and Brun, J.-P., 1997, Granite intrusion along strike-slip zones in experiment and nature: *American Journal of Science*, v. 297, p. 651–678.
- Rutter, E.H., Faulkner, D.R., Brodie, K.H., Phillips, R.J., and Searle, M.P., 2007, Rock deformation processes in the Karakoram fault zone, Eastern Karakoram, Ladakh, NW India: *Journal of Structural Geology*, v. 29, p. 1315–1326, doi: 10.1016/j.jsg.2007.05.001.
- Sawyer, E.W., 1999, Criteria for the recognition of partial melting: *Physical and Chemistry of the Earth, Ser. A*, v. 24, no. 3, p. 269–279, doi: 10.1016/S1464-1895(99)00029-0.
- Searle, M.P., Weinberg, R.F., and Dunlap, W.J., 1998, Transpressional tectonics along the Karakoram fault zone, northern Ladakh, in Holdsworth, R.E., and Strachan, R.A., eds., *Continental Transpressional and Transtensional Tectonics*: Geological Society of London Special Publication 135, p. 307–326.
- Tikoff, B., and Teyssier, C., 1992, Crustal-scale, en-echelon “P-shear” tensional bridges: A possible solution to the batholithic room problem: *Geology*, v. 20, p. 927–930, doi: 10.1130/0091-7613(1992)020<0927:CSEEPS>2.3.CO;2.
- Valli, F., Nicolas, A., Leloup, P.H., Sobel, E.R., Maheo, G., Lacassin, R., Guillot, S., Li, H., Tapponnier, P., and Xu, Z., 2007, Twenty million years of continuous deformation along the Karakoram fault, western Tibet: A thermochronological analysis: *Tectonics*, v. 26, p. TC4004, doi: 10.1029/2005TC001913.
- Valli, F., Leloup, P.H., Paquette, J.-L., Arnaud, N., Li, H., Tapponnier, P., Lacassin, R., Guillot, S., Liu, D., Deloule, E., Xu, Z., and Maheo, G., 2008, New U-Th/Pb constraints on timing of shearing and long-term slip-rate on the Karakoram fault: *Tectonics*, doi: 10.1029/2007TC002184 (in press).
- Vigneresse, J.L., 1995, Control of granite emplacement by regional deformation: *Tectonophysics*, v. 249, p. 173–186, doi: 10.1016/0040-1951(95)00004-7.
- Weinberg, R.F., 1999, Mesoscale pervasive melt migration: Alternative to dyking: *Lithos*, v. 46, no. 3, p. 393–410, doi: 10.1016/S0024-4937(98)00075-9.
- Weinberg, R.F., and Dunlap, W.J., 2000, Growth and deformation of the Ladakh Batholith, northwest Himalayas: Implications for timing of continental collision and origin of calc-alkaline batholiths: *The Journal of Geology*, v. 108, p. 303–320, doi: 10.1086/314405.
- Weinberg, R.F., and Mark, G., 2008, Magma migration, folding and disaggregation of migmatites in the Karakoram shear zone, Ladakh, NW India: *Geological Society of America Bulletin*, v. 120, 7/8, 994–1009, doi: 10.1130/B26227.1.
- Weinberg, R.F., and Searle, M.P., 1998, The Pangong injection complex, Indian Karakoram: A case of pervasive granite flow through hot viscous crust: *Journal of the Geological Society of London*, v. 155, p. 883–891, doi: 10.1144/gsjgs.155.5.0883.
- Weinberg, R.F., Dunlap, W.J., and Whitehouse, M., 2000, New field, structural and geochronological data from the Shyok and Nubra valleys, northern Ladakh: Linking Kohistan to Tibet, in Khan, A., Treloar, P.J., and Searle, M.P., eds., *Tectonics of the Nanga Parbat Syn-taxis and the Western Himalaya*: Geological Society of London Special Publication 170, p. 253–275.
- Weinberg, R.F., Sial, A.N., and Mariano, G., 2004, Plutons and shear zones in the Borborema Province, Brazil: *Geology*, v. 32, p. 377–380, doi: 10.1130/G20290.1.

MANUSCRIPT RECEIVED 4 NOVEMBER 2007

REVISED MANUSCRIPT RECEIVED 12 FEBRUARY 2008

MANUSCRIPT ACCEPTED 29 FEBRUARY 2008

PRINTED IN THE USA